Neural basis of interaction between target presence and display homogeneity in visual search: An fMRI study

Ping Wei [a,b,c,d], Hermann J. Müller [d], Stefan Pollmann [e], Xiaolin Zhou [a,b,c,*]

[a] [illegible] 100[illegible]71, [illegible]
[b] [illegible] 100[illegible]71, [illegible]
[c] [illegible] 100[illegible]71, [illegible]
[d] [illegible] -[illegible]0[illegible]02 [illegible]
[e] [illegible] -3[illegible] 016 [illegible]

---

article info

[illegible]
Received 19 June 2008
Revised 29 November 2008
Accepted 23 December 2008
Available online 8 January 2009

[illegible]
Visual search
Feature search
Display homogeneity
fMRI

abstract

The functional magnetic resonance imaging (fMRI) technique was used to investigate the functional neuroanatomy of the attention mechanisms employed in visual search with homogeneous or heterogeneous displays. Participants were asked to search for a vertically oriented bar among distractor bars with the same or different orientations, with half of the trials being target-present and the other half being target-absent. Behaviorally, RTs were slower for target-absent than for -present trials when the distractors were heterogeneous, but were faster for target-absent than for -present trials when the distractors were homogeneous. At the neural level, a widely distributed brain network was involved in this interaction. The bilateral frontal eye fi

threshold, or when none of the item identities activated in parallel reaches the threshold (Horowitz and Wolfe, 1998). A target-absent response can also be made as soon as the observer finds the display to be homogeneous (Chun and Wolfe, 1996).

Thus, the way the search display is composed may impact upon the strategy for deciding “target-absent”, leading to differential RT patterns for different types of search display. The computational

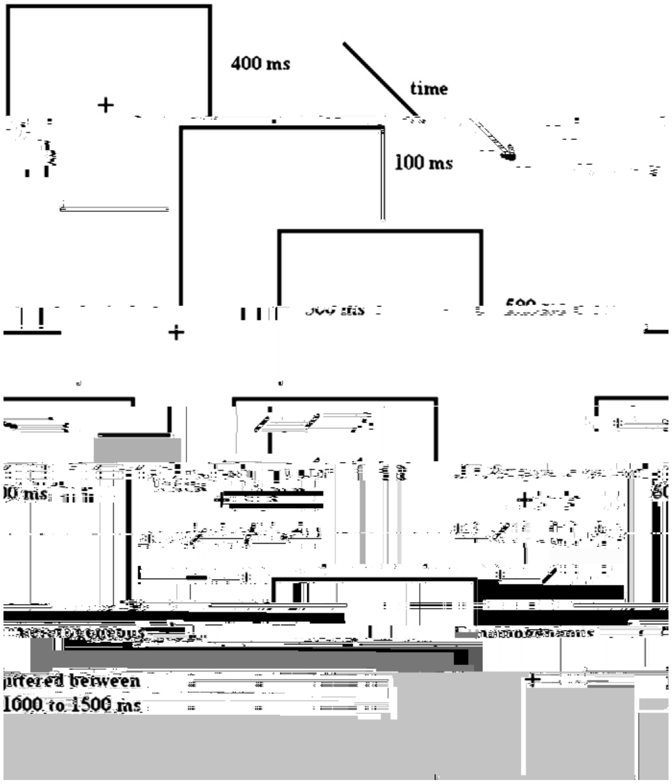

Fig. 1. An example trial sequence with a target present in a heterogeneous or homogeneous search display. Stars (not shown in the real search display) in the display examples here are the remaining 4 positions after 8 were randomly selected from the total 12 possible positions for search items to be displayed.

Stimuli were presented through an LCD projector onto a rear projection screen located behind the participant's head. Participants viewed the screen through an angled mirror on the head-coil. Presentation of the stimuli and recording of the responses were controlled by the Presentation software (http://nbs.neuro-bs.com/). At the start of each trial, a white fixation cross, measuring 0.20° of visual angle, appeared at the center of the black screen for 1000 ms. A black screen of 100 ms was inserted 400 ms after the onset of the fixation sign, so that the cross appeared to flash briefly. This was to warn participants about the upcoming search display, which was presented for 500 ms. The search display consisted of a central fixation marker surrounded by 8 bar stimuli (each measuring 0.8 × 0.2° in visual angle). The stimuli were placed at 8 (randomly selected) positions on a virtual, cross-shaped grid, with a maximum eccentricity of 3° of visual angle (see Fig. 1 for trial sequence and sample display).

Each experimental condition consisted of 48 trials, intermixed with 48 null trials on which only the fixation cross was presented. The four experimental conditions and null trials were randomized in one continuous scanning session of 12 min and 7.5 s. Only the fixation sign was displayed during the first 7.5 s for participants to become accustomed to the scanning noise and for the MR signal to reach a steady state. All participants completed a training session of 10 min before the scanning.

[illegible]

A 3T Siemens Trio system with a standard head coil at the MRI Center for Brain Research in Beijing Normal University was used to obtain T2*-weighted echo-planar images (EPI) with blood oxygenation level-dependent (BOLD) contrast (matrix size: 64 × 64, pixel size: 3.4 × 3.4 mm). Twenty-four transversal slices oriented parallel to anterior and posterior commissures of 4 mm thickness that covered the whole brain were acquired sequentially in ascending order with a 1 mm gap (TR = 1.5 s, TE = 30 ms, FOV = 220 mm, flip angle = 90°). The first five volumes were discarded to allow for T1 equilibration effects. Images were spatially realigned to the sixth volume for head movement correction, interpolated in time (temporal realignment to the middle slice for slice acquisition order correction), and normalized to a standard EPI template (Montreal Neurological Institute template provided by Statistical Parametric Mapping [SPM], see below) with resample of 2 × 2 × 2 mm^3 voxels. Data were then smoothed with a Gaussian kernel of 8 mm full-width half-maximum to accommodate inter-subject anatomical variability.

[illegible]

Data were analyzed by using Statistical Parametric Mapping software SPM2, Wellcome Department of Imaging Neuroscience, London (Friston et al., 1995), employing a random-effects model. At the first level, four event types were defined, including: target-absent trials for heterogeneous displays (Het_ab), target-present trials for heterogeneous displays (Het_pre), target-absent trials for homogeneous displays (Hom_ab), and target-present trials for homogeneous displays (Hom_pre).The event type was time-locked to the onset of the search display by a canonical synthetic hemodynamic response function (HRF). Additionally, all error trials were included as an extra regressor of no interest. The obtained contrast images of the first-level analysis were entered into a second level random-effects group analysis. The activations will be reported at a family-wise error (FWE) corrected threshold of [illegible] < 0.05.

Moreover, to examine in detail how the activated brain areas were modulated by display homogeneity and target-presence, we carried out a region-of-interest (ROI) analysis by extracting beta values from the peak voxels in the activated brain areas (see Table 2 for exact locations).

Results

[illegible]

Mean reaction times (RTs) and response error rates were calculated for each of the participants. As can be seen in Table 1, the error rates were higher for target-present (target misses) than for target-absent trials (false alarm), suggesting that participants tended to terminate the search prematurely and therefore miss the target. To correct for the potential speed-accuracy tradeoffs, we carried out a “kill-the-twin” procedure (Eriksen, 1988; Grice et al., 1977). The logic is that if participants have a tendency to respond “no” in a fast guess manner, thus generating faster correct-rejection RTs on target-absent trials and target-miss errors on -present trials, then eliminating correct-rejection trials whose RTs are “twins” of target-miss RTs would correct the mean RT estimate for the correct-rejection trials. Similarly, if participants have a tendency to respond “yes” in a fast-guess manner, thus generating faster correct-hit RTs on target-present trials and false-alarms on -absent trials, then eliminating correct-hit trials whose RTs are the “twins” of false-alarm RTs would correct the mean RT estimate for the correct-hit trials. In the present analysis, twins of error RTs were computed by searching for an RT in correct-

Table 1
Mean reaction times (ms), standard deviations, and error percentages (%) as a function of display homogeneity and target presence

	Heterogeneous		Homogeneous	
	Target-absent	Target-present	Target-absent	Target-present
RT	770 (767)	661 (660)	560 (560)	580 (580)

rejection or correct-hit trials which corresponded to an error RT (within a range of ±3 ms) on target-miss or false-alarm trials, respectively. These “twins” RTs were then removed from the “correct” data set. This procedure was carried out separately for heterogeneous and homogeneous displays for each participant, which led to the elimination of 2.0% of the data in total. As can be seen from Table 1, RT performance did not change as a result of removing the error “twins”, indicating that the RT data were largely undistorted by possible speed-accuracy tradeoffs.

The remaining data were then trimmed by deleting outlier RTs that were more than three standard deviations above or below the mean in each experimental condition (1.2% of the data in total). A 2 (homogeneous vs. heterogeneous) × 2 (target absent vs. present) analysis of variance (ANOVA) was then conducted, which revealed both main effects to be significant: display homogeneity, $(1, 15) = 102.79$, $< .001$, and target presence, $(1, 15) = 11.41$, $< .005$. RTs were slower to heterogeneous than to homogeneous display (714 vs. 570 ms), and overall slower to target-absent than to target-present trials (664 vs. 620 ms). As can be seen from Fig. 2

the display was homogeneous ($p < .001$ for all the regions), but comparable or larger beta values for target-absent and -present trials for heterogeneous display (for right IPS and SEF, the beta values were larger for target-absent trials, $p < .05$). Moreover, while beta values showed little change for target-present trials as a function of homogeneity ($p < .05$ for left FEF, but $p > .1$ for all the other regions), they were significantly decreased for target-absent trials when displays were homogeneous ($p < .001$ for all the regions).

[illegible]

1993), with a significant interaction between display homogeneity and target presence. RTs were faster for target-absent than for -present displays when the distractors were homogeneous; in contrast, RTs were slower for target-absent than for -present displays when the distractors were heterogeneous. The speed with which a target was detected depended not only on how much it differed from the surrounding distractor items, but also on the homogeneity among the distractors. According to the SERR model (e.g., Humphreys and Müller, 1993), the processing system evaluates the homogeneity of the display, which allows for faster rejection of distractor groups in the case of homogeneous distractors.

At the neural level, the present experiment revealed a set of brain regions sensitive to display homogeneity. More importantly, it demonstrated that bilateral FEF, IPS, precentral gyrus, and SEF were also involved in the interaction between display homogeneity and target presence, with positive activations in these regions. In addition, SFG and TPJ showed a significant interaction, but with negative signal changes. Furthermore, the patterns of estimated activations in these regions were generally parallel to the pattern of the RT interaction, with little difference in signal strength between homogeneity conditions for target-present trials and larger increases from homogeneous to heterogeneous displays for target-absent trials. In the following paragraphs, we discuss these brain activations in relation to the cognitive processes in visual search.

[illegible]

The activated dorsal brain areas, including bilateral FEF, IPS, precentral gyrus, as well as SEF, showed consistent activation patterns, with roughly equivalent activations for the heterogeneous target-present and -absent trials as well as homogeneous target-present trials (Fig. 4). In these conditions, target template matching is necessary for making proper responses. In contrast, a “no” response can be quickly made to a homogeneous target-absent display; the absence of any visual irregularity permits all display items to be rejected together, with no need for template matching of the target. Therefore, it is likely that the activated dorsal brain regions are responsible for template matching in visual target selection.

Concerning the specific role of IPS and FEF in visual search, previous studies have found overlap of activation in these areas for conjunction search and difficult feature search (Donner et al. 2002, 2003; Leonards et al. 2000), suggesting a common target representation or selection mechanism engaged in different types of visual search. For example, Donner et al. (2003) reported that the anterior IPS and IPTO (junction

Müller, H.J., Humphreys, G.W., Olson, A.C., 1998. SEarch via Recursive Rejection (SERR). In: Wright, R.D. (Ed.), Visual Attention. Vancouver Studies in Cognitive Science, Vol. 8. Oxford University Press, New York, pp. 389–416.

Müller-Plath, G., Pollmann, S., 2003. Determining subprocesses of visual feature search with reaction time models. Psychol. Res. 67, 80–105.

Niebur, E., Koch, C., Rosin, C., 1993. An oscillation-based model for the neuronal basis of attention. Vis. Res. 18, 2789–2802.

Nobre, A.C., Coull, J.T., Walsh, V., Frith, C.D., 2003. Brain activations during visual search: contributions of search efficiency versus feature binding. NeuroImage 18, 91–103.

Pollmann, S., Cramon, D.Y., 2000. Object working memory and visuospatial processing: functional neuroanatomy analyzed by event-related fMRI. Exp. Brain Res. 133, 12–22.

Pollmann, S., Wiggins, C.J., Norris, D.N., von Cramon, D.Y., Schubert, T., 1998. Use of short intertrial intervals in single-trial experiments: a 3T-fMRI-study. NeuroImage 8, 327–339.

Raichle, M.E., Gusnard, D.A., 2002. Appraising the brain's energy budget. Proc. Natl. Acad. Sci. 99 (16), 10237–10239.

Raichle, M.E., MacLeod, A.M., Snyder, A.Z., Powers, W.J., Gusnard, D.A., Shulman, G.L., 2001. A default mode of brain function. Proc. Natl. Acad. Sci. 98, 676–682.

Rushworth, M.F.S., Paus, T., Sipila, P.K., 2001. Attention systems and the organization of the human parietal cortex. J. Neurosci. 21, 5262–5271.

Sato, T.R., Watanabe, K., Thompson, K.G., Schall, J.D., 2003. Effect of target-distractor similarity on FEF visual selection in the absence of the target. Exp. Brain Res. 151, 356–363.

Schubö, A., Schröger, E., Meinecke, C., 2004. Texture segmentation and visual search for pop-out targets. An ERP study. Cogn. Brain Res. 21, 317–334.

Schubö, A., Wykowska, A., Müller, H.J., 2007. Detecting pop-out targets in contexts of varying homogeneity: investigating homogeneity coding with event-related brain potentials. Brain Res. 1138, 136–147.

Serences, J.T., Shomstein, S., Leber, A.B., Golay, X., Egeth, H.E., Yantis, S., 2005. Coordination of voluntary and stimulus-driven attentional control in human cortex. Psychol. Sci. 16, 114–122.

Shulman, G.L., 1997. Common blood flow changes across visual tasks: II. decreases in cerebral cortex. J. Cogn. Neurosci. 9, 648–663.

Shulman, G.L., McAvoy, M.P., Cowan, M.C., Astafiev, S.V., Tansy, A.P., d'Avossa, G., Corbetta, M., 2003. Quantitative analysis of attention and detection signals during visual search. J. Neurophysiol. 90, 3384–3397.

Shulman, G.L., Astafiev, S.V., McAvoy, M.P., d'Avossa, G., Corbetta, M., 2007. Right TPJ deactivation during visual search: functional significance and support for a filter hypothesis. Cereb. Cortex 17, 2625–2633.

Todd, J.J., Fougnie, D., Marois, R., 2005. Visual short-term memory load suppresses temporo-parietal junction activity and induces inattentional blindness. Psychol. Sci. 16, 965–972.

Tomasi, D., Ernst, T., Caparelli, E.C., Chang, L., 2006. Common deactivation patterns during working memory and visual attention tasks: an intra-subject fMRI study at 4 Tesla. Hum. Brain Mapp. 27, 694–705.

Treisman, A.M., 1988. Features and objects: the fourteenth Bartlett memorial lecture. Q. J. Exp. Psychol. 40, 201–237.

Treisman, A.M., Gelade, G., 1980. Feature-integration theory of attention. Cogn. Psychol. 12, 97–136.

Wilkinson, D.T., Halligan, P.W., Henson, R.N.A., Dolan, R.J., 2002. The effects of interdistracter similarity on search processes in superior parietal cortex. NeuroImage 15, 611